

Kochi Chapter

Indian Geotechnical Conference

IGC 2022

15th – 17th December, 2022, Kochi

Numerical Analysis of Reinforced Ring Foundation Subjected to Eccentric-Inclined Loading

Kishan Kumar¹, Subhadeep Metya^{1[0000-0003-0622-6978]} and Gautam Bhattacharya

¹ National Institute of Technology Jamshedpur, Jharkhand 831014
smetya.ce@nitjsr.ac.in

Abstract. Reinforced earth forms one of the ground improvement techniques using in-situ soil reinforcement for purposes of improving the strength and stiffness of soil, for instance, the use of Geosynthetics to increase the bearing capacity and decrease the settlement of foundations. In the past, various researches have been conducted to study the behavior of reinforced soil under various types of footings and loading conditions. However, the behavior of reinforced ring foundation is still a relatively unexplored area. But its use in geotechnical engineering is an economically viable alternative to circular foundation. Furthermore, it is used in a variety of special structures such as cooling towers, silos and oil storages, transmission towers etc. In the present study, numerical analyses of reinforced ring foundation subjected to eccentric-inclined loading have been performed using PLAXIS 3D. It has been observed that with the eccentric-inclined loading, the design of ring foundation may be permitted up to the ratio of internal to external radii of 0.1875 without compromising the bearing capacity of circular foundation with equal external diameter. The effect of soil reinforcement has been found to be the maximum when the depth of the first layer of reinforcement is kept within the range of $(0.2B - 0.4B)$, where B is the outer diameter of the ring foundation.

Keywords: Geosynthetics, Ring foundation, Numerical analysis (FEM), PLAXIS 2D, Eccentric-inclined loading.

1 Introduction

Ring foundation is a type of annular foundation most suitable for a variety of special structures such as cooling towers, silos and oil storages, chimneys, transmission towers, elevated tanks etc. Unlike strip, rectangular and square footings, circular and ring footings have no weak corners and hence no stress concentration occurs in these foundations. In terms of economy, a ring foundation is preferable to a circular foundation (wherever possible) because of less material requirement for its construction as compared with circular foundation. Also, the kern distance is larger for ring foundation as compared to circular foundation. Further, the bearing capacity and settlement analyses for ring foundation, especially the reinforced ring foundation, is not as well established as it is for strip, square, rectangular and circular foundations.

Based on their research on reinforced ring foundation, Guido et al. [6] and Laman and Yildiz [12] noted that as the tensile strength of the geogrid reinforcement increas-

es, the bearing capacity ratio (BCR) of reinforced ring foundation (defined as the ratio of the bearing capacities of the reinforced and unreinforced foundations) also increases. As the number of reinforcing layers (N) is increased, the BCR continues to increase up to a certain value of N , after which the increase becomes negligible. Laman and Yildiz [11, 12] observed that bearing capacity (BC) increases with increase in stiffness of the reinforcement. They also noted that effective depth obtained in their study was $1.0B$ for ring foundation. Basudhar et al. [2] noted that rectangular shaped geogrid is favorable as compared to circular one with respect to material saving. They also noted that B.C. increases substantially for each extra geogrid layer, but the settlement at failure didn't change appreciably. Badakhshan and Noorzad [1] observed that as the eccentricity of circular and square footing with eccentric loading increases, the ultimate load and settlement at ultimate load decreases. Badakhshan and Noorzad [1] also noted that with increase in load eccentricity, reinforcement layers have more influence on circular footing than square footing. Hosamo et al. [7] noted that bearing capacity ratio of ring foundation decreases as the spacing between geogrid layers (h) is increased. Further they noted that $n (= r/R)$ value between 0.5 and 0.8 give optimum BC increase in ring footing. In summary, it has been observed that few studies have been reported in the past with concentric or eccentric loading (Boushehrian and Hataf [3]; Chakraborty and Kumar [4]; Choobbasti et al. [5]; Ismael [8]; Keshavarz and Kumar [9]; Laman and Yildiz [11]; Sharma and Kumar [13]). To the best of authors knowledge, no studies have been reported with inclined-eccentric loading. However, in real life, the applied loading on the foundations is seldom vertical and concentric. Therefore, further studies on ring foundation on reinforced soil is necessary to understand and quantify the improvement in bearing capacity and decrement in settlement.

Based on the literature review presented above, the point-wise objectives of the present study are: (1) to develop a numerical model in PLAXIS 3D using the studies reported in Laman and Yildiz [11, 12] and validate the same; (2) to observe the behavior of a geogrid reinforced ring foundation subjected to inclined and eccentric loading by analyzing the soil displacement pattern and effective stress variation in PLAXIS 3D; and (3) to study the variation of bearing capacity ratio (BCR) of a ring foundation under the influence of eccentrically inclined load with variations in seven parameters namely, radius ratio of the ring footing (r/R or n), number of geogrid layers below the footing (N), the first layer depth of reinforcement from the footing base (u), the spacing between reinforcing layers (h), the width of reinforcement layer (b), the load eccentricity (e) and the load inclination (i).

2 Analysis Methods and Illustrative Example

The example problem considered in the present study concerns a ring foundation with outer diameter (B) of 85 mm and thickness (t) of 20 mm at the surface of a layer of sand. The boundaries of the soil medium are kept equal to the dimensions of the tank designed for experimentation by Laman and Yildiz [11] (i.e., 700 mm x 700 mm x 700 mm). The general layout of geogrid reinforced foundation system considered in the present study is shown in Fig. 1 and has been developed in PLAXIS 3D.

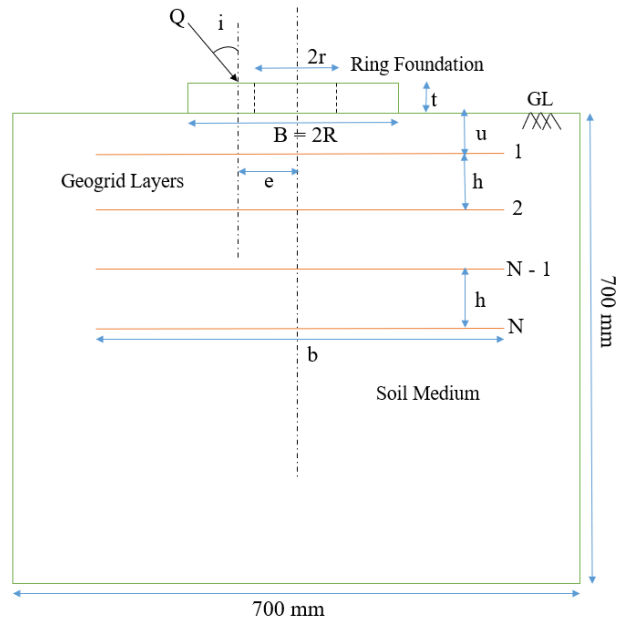


Fig. 1. Schematic diagram of ring foundation with eccentric-inclined loading

Table 1. Soil parameters used in PLAXIS 3D modelling (Laman and Yildiz [12])

Sl. No.	Parameter	Value
1.	Unit weight of soil γ_s (kN/m ³)	17.1
2.	Secant stiffness E_{50} (kN/m ²)	28000
3.	Friction angle ϕ (degrees)	41
4.	Cohesion c (kN/m ²)	0.3
5.	Dilatancy angle ψ (degrees)	11
6.	Earth pressure at rest (K_0)	0.34
7.	Poisson's ratio	0.2

As reported by Laman and Yildiz [11, 12], uniform and fine sand was taken from the Seyhan river bed in Turkey and that was tested in the laboratory. The dry unit weight of the sand was found out to be 17.1 kN/m³. The angle of shearing resistance using direct shear tests was found out to be 41°. For the purpose of modeling the sand, an elasto-plastic hyperbolic model called the hardening soil model (HSM) was selected for the non-linear sand behavior since it was found out that results obtained by other material models such as linear elastic and Mohr-Coulomb was not in good agreement with the experimental findings. The HSM parameters used to model the soil is shown in the Table 1. The footing and geogrid parameters can be referred to Tables 2 and 3 respectively.

Table 2. Footing parameters used in PLAXIS 3D modelling (Laman and Yildiz [12])

Sl. No.	Parameters	Value
1.	Thickness, t (mm)	20
2.	Modulus of elasticity, E (kN/m ²)	207×10^6
3.	Unit weight of steel, γ_p (kN/m ³)	7850
4.	Poisson's ratio of steel, ν	0.25

Table 3. Geogrid parameters used (Laman and Yildiz [12]).

Sl. No.	Parameters	Values
1.	EA (kN/m)	465
2.	GA (kN/m)	232.5

Table 4 summarizes the parameters that are varied in the various parametric studies conducted in this paper while keeping all the other parameters at their mean values.

Table 4. Parameters used in different parametric study

Studies conducted	Parameter	Mean value	Range considered
Study 1	r/R	0.375	0 to 0.75
Study 2	u/B	0.6	0.2 to 1
Study 3	h/B	0.6	0.2 to 1
Study 4	N	3	1 to 5
Study 5	b/B	3	1 to 5
Study 6	e/B	0.25	0 to 0.5

The validation has been done by comparing the results obtained in PLAXIS 3D and those observed by Laman and Yildiz [12] both for unreinforced and reinforced cases. However, because of the limitation of the page number, those figures with further details are not given in this paper and the readers can refer to reference [10].

3 Results and Discussion

As already mentioned, in this paper, several parametric studies have been conducted to observe the nature of variations in the bearing capacity of the geogrid reinforced ring foundation subjected to inclined and eccentric loading due to the variation in seven parameters namely, ratio of internal to external radii of ring foundation (r/R), ratio of the depth of first layer geogrid to external diameter of footing (u/B), ratio of inter-layer distance in successive geogrid layers to the external diameter of footing (h/B), number of geogrid layers (N), ratio of width of geogrid layer to the external diameter of footing (b/B), inclination of loading (i) and ratio of eccentricity of loading to the external diameter of footing (e/B).

3.1 Study 1: Effect of Size of Ring Footing

In study 1, to observe the effect of the size of ring foundation on its bearing capacity, the ratio of internal to external radii of ring foundation (r/R) has been varied from 0.0 to 0.75 keeping the other parameters constant at their mean values as in Table 4. The variations of bearing capacity ratios (BCR) with the changes in r/R values are shown in Fig. 2.

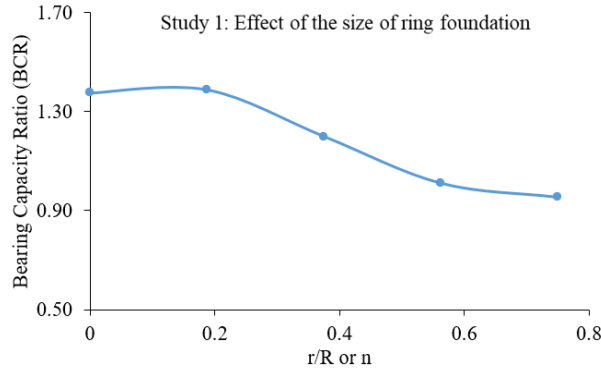


Fig. 2. Variations of bearing capacity ratios (BCR) with the variation in ring size (r/R)

From Fig. 2, the following points have been observed.

- (1) BCR increases slightly from $r/R = 0$ to 0.1875 and then decreases thereafter almost linearly. The decrease in bearing capacity value with increase in size (n value) from 0 to 0.75 has been observed to be from 131 to 63 kN/m^2 in unreinforced case and 180 to 60 kN/m^2 in reinforced case with a given eccentric inclined loading.
- (2) Further, it becomes evident that with the eccentric-inclined loading, the design of ring foundation may be permitted with r/R of 0.1875 without compromising the bearing capacity of circular foundation with equal external diameter.
- (3) For n value up to 0.5625, the values of the bearing capacity (BC) of reinforced soil are greater than that of unreinforced soil. For $n > 0.5625$, no beneficial effect of geogrid has been observed in increasing the BC of the soil.
- (4) From Figs. 3 and 4, it is evident that the immediate settlement value has decreased in unreinforced case from $n = 0$ to $n = 0.1875$. Figs. 5 and 6 shows that displacement pattern is more uniform in reinforced ring footing with $n = 0.1875$ as compared with pure circular footing.
- (5) On reinforcing the ring foundation system with $n = 0.5625$, the immediate settlement is decreasing. However, there is not much appreciable change in z -direction displacement contour pattern and hence, it has been observed that BCR value at $n = 0.5625$ is equal to 1 (Figs. 7 and 8).

3.2 Study 2: Effect of Depth of First Layer of Geogrid

In study 2, to observe the effect of depth of first layer of geogrid (from ground level) on its bearing capacity, the ratio of the depth of first layer of geogrid to width of foot-

ing has been varied from 0.2 to 1.0 keeping the other parameters constant at their mean values as in Table 4. The results of the variation in terms of its BCR is shown in Fig. 9.

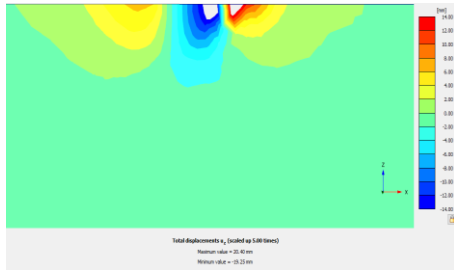


Fig 3. Vertical displacement contour (VDC) in unreinforced soil for $n = 0$

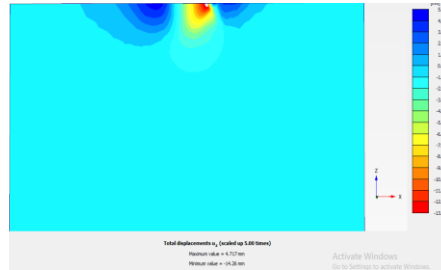


Fig 4. VDC in unreinforced soil for $n = 0.1875$

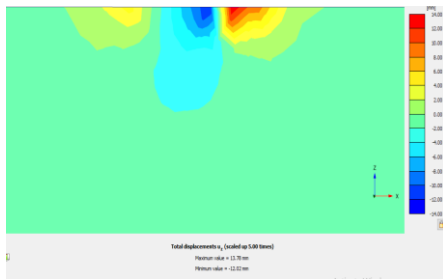


Fig 5. VDC in reinforced soil for $n = 0$

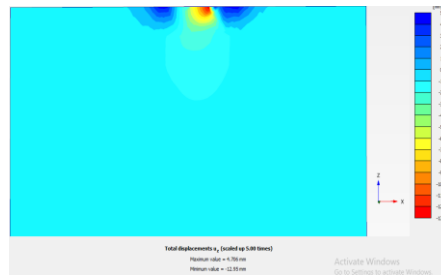


Fig 6. VDC in reinforced soil for $n = 0.1875$

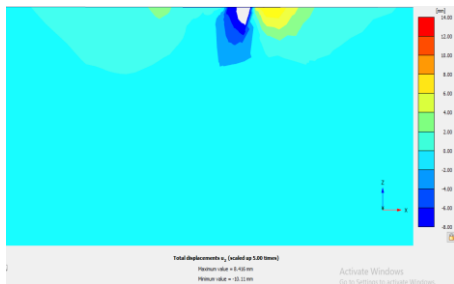


Fig. 7. VDC in unreinforced soil for $n = 0.5625$

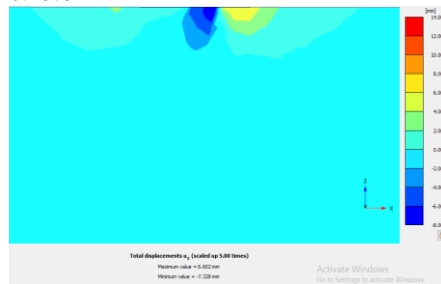


Fig. 8. VDC in reinforced soil for $n = 0.5625$

From Fig. 9, the following points have been observed.

- (1) For u/B value less than 0.4, an appreciable increase in bearing capacity is observed, while, for u/B value greater than 0.4, an approximate linear graph is obtained which is as good as an unreinforced foundation.
- (2) At u/B equal to 0.2, the bearing capacity ratio was observed to be greater than 4, but with increase in its value to 0.4, the Bearing capacity ratio decreases drastically to around 1.5. Further increase in u/B reduces the BCR near about 1. This shows that the effective depth for maximum increase in BCR to observe (d_{eff}) is about 0.2-0.4 times of B for the given loading condition.
- (3) Fig. 9 also shows that as the depth of first layer of geogrid (u) increases from u/B equal to 0.2 to 0.4, the BC of the ring foundation decreases considerably from 490

to 170 kN/m^2 . So, as the first geogrid layer is placed nearer to the footing base, the bearing capacity is observed to increase. It has also been observed that after $u/B = 0.6$, the effect of reinforcing the system has negligible effect in increasing the bearing capacity of the foundation.

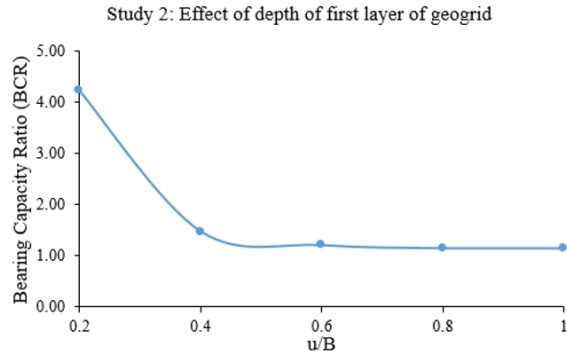


Fig. 9. Variation of BCR with the variation in depth of first layer of geogrid (u/B)

- (4) From Figs. 10 and 11, it is evident that the soil response with $u/B = 0.2$ is better than $u/B = 0.4$. This explains the observation that $u/B = 0.2$ gives higher bearing capacity value than $u/B = 0.4$.

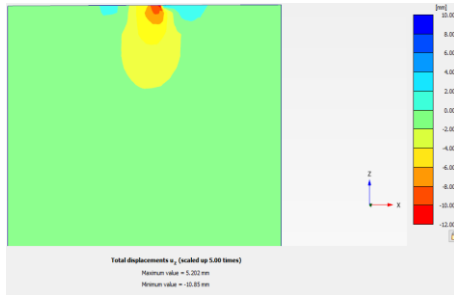


Fig 10. VDC in reinforced soil for $u/B = 0.2$

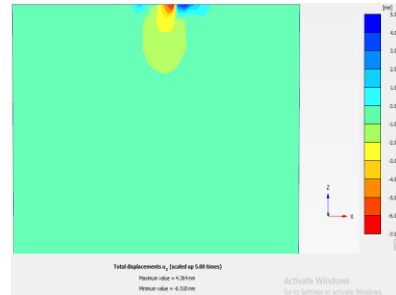


Fig. 11. VDC in reinforced soil for $u/B = 0.4$

3.3 Study 3: Effect of Inter-Layer Distance in Successive Geogrid Layers

In study 3, to observe the effect of inter-geogrid layer distance on its bearing capacity, the ratio of inter-geogrid layer distance and width of footing has been varied from 0.2 to 1.0 keeping the other parameters constant at their mean values as in Table 4. The results of the variation in terms of its BCR is shown in Fig. 12. The following points have been observed from the Fig. 12:

- (1) The BCR value decreases first from 0.2 to 0.4 but increases thereafter and becomes constant after $h/B = 0.6$. The bearing capacity value at first, decreases from 132 to 122 kN/m^2 and then increases from 122 to 140 kN/m^2 .
- (2) The optimum value of h/B from the observation came out to be 0.6.

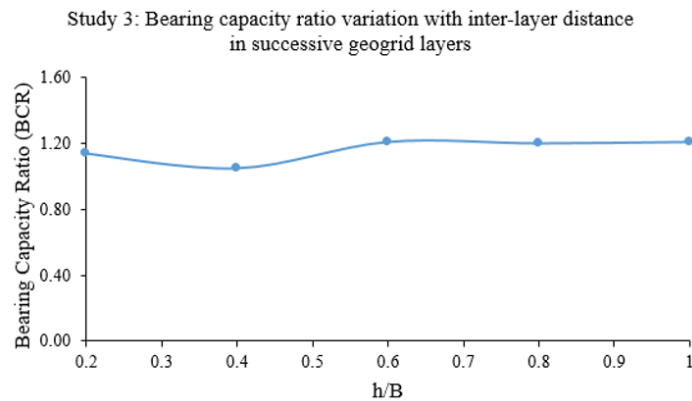


Fig. 12. Variation of BCR with the variation in inter-layer distance of successive geogrids (h/B)

3.4 Study 4: Effect of Variation of Number of Geogrid Layers

In study 4, to observe the effect of number of geogrid layers on its bearing capacity, the number of geogrid layers has been varied from 1 to 5 keeping the other parameters constant at their mean values as in Table 4. The results of the variation in terms of its Bearing Capacity Ratio is shown in Fig. 13.

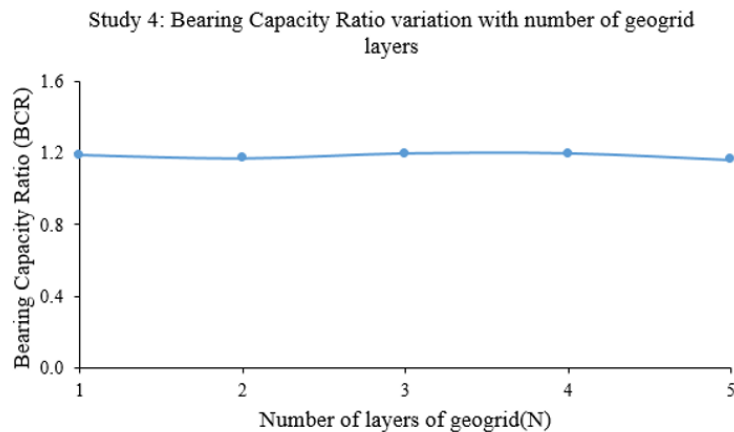


Fig. 13. Variation of BCR with the variation in number of layers of geogrids (N)

From Fig. 13, the following observations have been made.

- (1) As the number of geogrid layers is increased from one to two, there is slight decrease in bearing capacity ratio from 1.19 to 1.17. The corresponding value of bearing capacity decreases from 138 to 136 kN/m².
- (2) Further increase in number of geogrid layers from two to four, results in increasing the bearing capacity ratio from 1.17 to 1.20. The bearing capacity value increases from 136 to 139 kN/m².

- (3) If the value of N is increased further from four to five, slight decrease in bearing capacity ratio has been observed. The bearing capacity decreases from 139 to 135 kN/m^2 .

3.5 Study 5: Effect of Variation of Width of Geogrid Layers

In study 5, to observe the effect of the width of geogrid layer on its bearing capacity, the ratio of width of geogrid layers to the width of the footing has been varied from 1 to 5 keeping the other parameters constant at their mean values as in Table 4. The results of the variation in terms of its bearing capacity ratio are shown in Fig. 14.

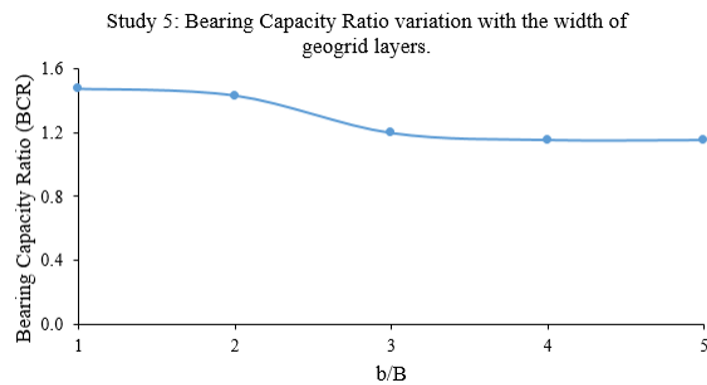


Fig. 14. Variation of BCR with the variation in width of the geogrid layers (b/B)

From Fig. 14, the following observations have been noted.

- (1) The bearing capacity ratio decreases from 1.47 to 1.16 as the width of the geogrid layer has been increased from B to $5B$. The corresponding decrease in bearing capacity value was from 171 to 134 kN/m^2 .
- (2) The bearing capacity ratio has been observed to be approximately constant after $b/B > 3$. Therefore, the optimum value of b/B obtained in the present study is 1.
- (3) It has been observed (from Figs. 15 and 16) that the displacement at failure has decreased considerably for $b/B = 3$ as compared to when the ratio was 2 at the same load. This accounts for the fact that the bearing capacity has decreased from 166 to 139 kN/m^2 while increasing b/B from 2 to 3.

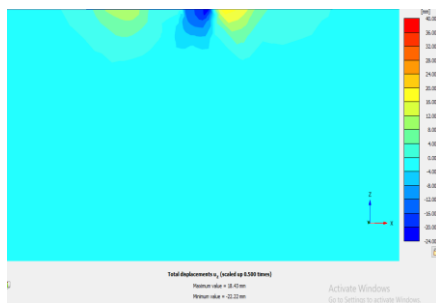


Fig. 15. VDC in reinforced soil for $b/B = 2$

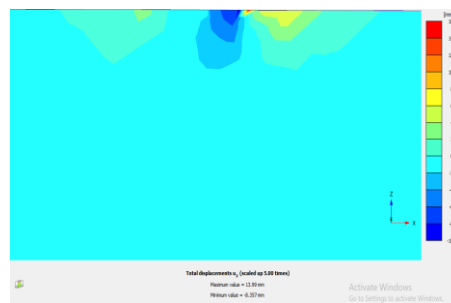


Fig. 16. VDC in reinforced soil for $b/B = 3$

3.6 Study 6: Effect of Variation of Load Eccentricity and Inclination

In study 6, to observe the effect of the load eccentricity and inclination in ring footing on its BC, the ratio of eccentricity and width of footing has been varied from 0.0 to 0.5 keeping the other parameters constant at their mean values as in Table 4. The results of the variation in terms of its Bearing Capacity Ratio is shown in Fig. 17. From Fig. 17, the following observations have been made.

- (1) Fig. 17 shows the successive decrease in bearing capacity ratio as e/B value increases, and it converges to 1 for e/B equal to 0.5. That is, when eccentricity equals half of the ring foundation width, then there is no effect of reinforcing the foundation system.
- (2) The bearing capacity for unreinforced case decreases non-linearly from 310 kN/m^2 for $e/B = 0$ to 36 kN/m^2 with $e/B = 0.5$. For the reinforced case, the corresponding decrease is from 484 kN/m^2 for $e/B = 0$ to 36 kN/m^2 for $e/B = 0.5$.
- (3) From the settlement values at failure from Figs. 18, 19, 20 and 21, it can be clearly seen that the soil response pattern is better for $e/B = 0$ as compared with $e/B = 0.5$. Hence, it has been observed in Fig. 17 that as eccentricity of loading has increased, the bearing capacity ratio has decreased.
- (4) It may be noted that the first three values of e/B i.e., 0, 0.125 and 0.25 are inside the kern distance (i.e., 24 mm from the value $(D_2+d_2)/4D$) and rest two point are outside the kern distance.

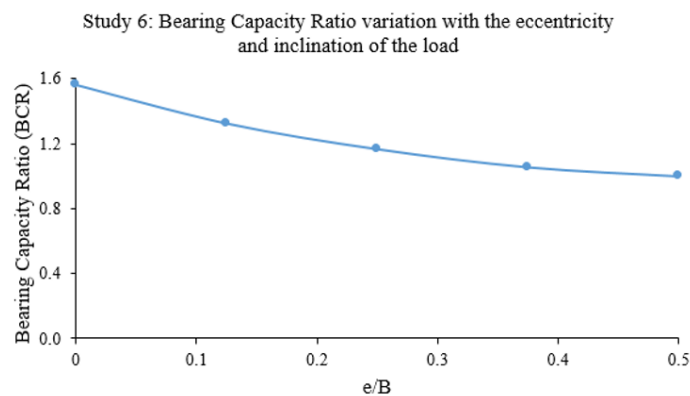


Fig. 17. Variation of BCR with the variation in load eccentricity and inclination

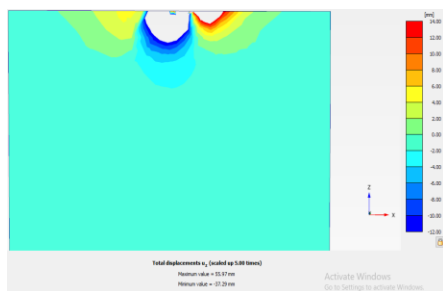


Fig.18. VDC in unreinforced soil for $e/B = 0$

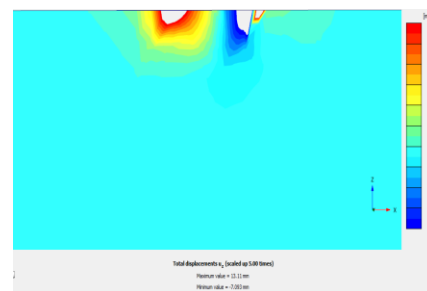


Fig. 19. VDC in unreinforced soil for $e/B = 0.5$

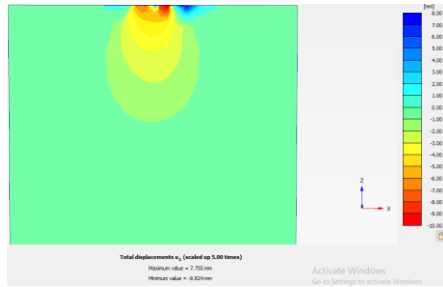


Fig. 20. VDC in reinforced soil for $e/B = 0$

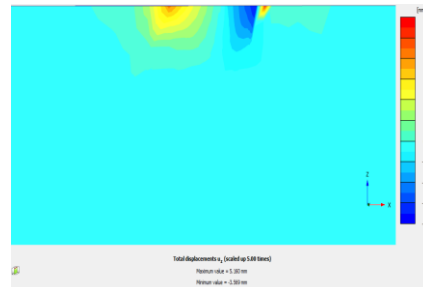


Fig. 21. VDC in reinforced soil for $e/B = 0.5$

4 Conclusions

A comprehensive numerical simulation has been performed to analyze the behavior of a ring footing model over reinforced and unreinforced sand, including identification of the dominant parameters to be considered in design. Based on the observations from the research work undertaken in this paper, the following concluding remarks can be made:

- (1) It has been observed that as the internal radius (r) of the ring foundation is increased, or in other words, the effective width of the ring is decreased, there is a decrease in the time to failure. This also indicates that the mode of failure changes from general shear failure (GSF) to punching shear failure (PSF). The settlement pattern becomes more uniform with the introduction of geogrid as soil reinforcement.
- (2) Further, it has been noted that with the eccentric-inclined loading, the design of ring foundation may be permitted up to the ratio of internal to external radii (r/R) of 0.1875 without compromising the bearing capacity of circular foundation with equal external diameter.
- (3) The effect of soil reinforcement has been found to be the maximum when the depth of the first layer of reinforcement is kept within the range of $(0.2B - 0.4B)$ (where B is the outer diameter of the ring foundation). It has been observed that the shear stress developed due to friction between soil and geogrid is also maximum for this condition.
- (4) With increase in the number of reinforcement layer (N), there is no appreciable increase in the bearing capacity ratio (BCR). This indicates that for the eccentric-inclined loading, only the first layer of reinforcement effectively contributes to the improvement in bearing capacity.
- (5) With increase in the eccentricity and inclination of the load, it is observed that the failure surface tends to move up from a position between the first layer and the second layer to a position above the first layer of the geogrid. This accounts for the fact that for higher values of eccentricity and inclination of the load, the contribution of geogrid as soil reinforcement towards improving the bearing capacity of the footing becomes negligibly small.
- (6) The effect of the depth of embedment of the footing is not considered in this study as it was observed by Sitharam and Sireesh [14] that increasing the em-

bedment depth increases the bearing capacity of the reinforced circular foundation system.

References

1. Badakhshan E, Noorzad A (2017) Effect of footing shape and load eccentricity on behavior of geosynthetic reinforced sand bed. *Geotext Geomembranes* 45:58–67. doi: 10.1016/j.geotextmem.2016.11.007
2. Basudhar PK, Saha S, Deb K (2007) Circular footings resting on geotextile-reinforced sand bed. *Geotext Geomembranes* 25:377–384. doi: 10.1016/j.geotextmem.2006.09.003
3. Boushehrian JH, Hataf N (2003) Experimental and numerical investigation of the bearing capacity of model circular and ring footings on reinforced sand. *Geotext Geomembranes* 21:241–256. doi: 10.1016/S0266-1144(03)00029-3
4. Chakraborty M, Kumar J (2014) Bearing capacity of circular foundations reinforced with geogrid sheets. *Soils Found* 54:820–832. doi: 10.1016/j.sandf.2014.06.013
5. Choobbasti AJ, Heshami S, Najafi A, Pirzadeh S, Farrokhzad F, Zahmatkesh A (2010) Numerical Evaluation of Bearing Capacity and Settlement of Ring Footing ; Case Study of Kazeroon Cooling Towers. *Int J Recent Res Appl Stud* 263–271
6. Guido VA, Chang DK, Sweeney MA (1986) Comparison of Geogrid and Geotextile Reinforced Earth Slabs. *Can Geotech J* 23:435–440. doi: 10.1139/t86-073
7. Hosamo H, Sliteen I, Ding S (2021) Numerical analysis of bearing capacity of a ring footing on geogrid reinforced sand. *Buildings* 11:1–12. doi: 10.3390/buildings11020068
8. Ismael NF (1996) Loading Tests on Circular and Ring Plates in Very Dense Cemented Sands. *J Geotech Eng* 122:281–287. doi: 10.1061/(asce)0733-9410(1996)122:4(281)
9. Keshavarz A, Kumar J (2017) Bearing capacity computation for a ring foundation using the stress characteristics method. *Comput Geotech* 89:33–42. doi: 10.1016/j.compgeo.2017.04.006
10. Kumar K (2022) Numerical and Sensitivity Analysis of Reinforced Ring Foundation Subjected to Eccentric-Inclined Loading. National Institute of Technology Jamshedpur, Jharkhand
11. Laman M, Yildiz A (2003) Model studies of ring foundations on geogrid-reinforced sand. *Geosynth Int* 10:142–152. doi: 10.1680/gein.2003.10.5.142
12. Laman M, Yildiz A (2007) Numerical studies of ring foundations on geogrid-reinforced sand. *Geosynth Int* 14:52–64. doi: 10.1680/gein.2007.14.2.52
13. Sharma V, Kumar A (2017) Influence of relative density of soil on performance of fiber-reinforced soil foundations. *Geotext Geomembranes* 45:499–507. doi: 10.1016/j.geotextmem.2017.06.004
14. Sitharam TG, Sireesh S (2004) Model studies of embedded circular footing on geogrid-reinforced sand beds. *Gr Improv* 8:69–75. doi: 10.1680/grim.8.2.69.36369